

Article

Solubility and Crystallization of Glucosamine Hydrochloride in Water with the Presence of Additives

 Zhiying Pan ¹, Yan Wang ¹ , Yang Xie ¹, Jie Tan ¹, Qian Zhang ², Jianxing Lu ², Shichao Du ^{1,*} 
 and Fumin Xue ^{1,*} 
¹ School of Pharmaceutical Sciences, Shandong Analysis and Testing Center, Qilu University of Technology (Shandong Academy of Sciences), Jinan 250014, China

² Shandong Runde Biotechnology Co., Ltd., Xintai 271200, China

* Correspondence: dushichao@tju.edu.cn (S.D.); xuefumin@qlu.edu.cn (F.X.)

Abstract: Glucosamine hydrochloride (GAH) is a kind of natural hexose, which is used to promote the synthesis of mucopolysaccharides and improve the metabolism of articular cartilage. In this paper, the solubility of GAH in pure water and aqueous system with the presence of three kinds of additives (HCl, NaCl, KCl) at temperatures ranging from 278.15 K to 323.15 K was determined by gravimetric method. When there are additives in water, the solubility of GAH increases with the increase of temperature and decreases with the increase of concentration of the three kinds of additives. When the additives were at similar mole fractions, HCl led to the lowest solubility of GAH. The modified Apelblat model and van't Hoff model were used to correlate the solubility data. The average relative deviation (ARD) data of Apelblat and van't Hoff models were less than 5%, indicating good fitting results. Based on the thermodynamic data, the cooling crystallization process of GAH was performed. It was found that the additives could affect the crystal morphology, particle size, and yield of GAH products. This study supplemented the thermodynamic data of GAH and studied the cooling crystallization process in the presence of GAH additives, which provided important guidance for the optimization of the crystallization process.

Keywords: glucosamine hydrochloride; additive; solubility; correlation; cooling crystallization



Citation: Pan, Z.; Wang, Y.; Xie, Y.; Tan, J.; Zhang, Q.; Lu, J.; Du, S.; Xue, F. Solubility and Crystallization of Glucosamine Hydrochloride in Water with the Presence of Additives. *Crystals* **2023**, *13*, 1326. <https://doi.org/10.3390/cryst13091326>

Academic Editor: Jaime Gómez Morales

Received: 9 August 2023

Revised: 24 August 2023

Accepted: 26 August 2023

Published: 30 August 2023



Copyright: © 2023 by the authors. Licensee MDPI, Basel, Switzerland. This article is an open access article distributed under the terms and conditions of the Creative Commons Attribution (CC BY) license (<https://creativecommons.org/licenses/by/4.0/>).

1. Introduction

Glucosamine hydrochloride (GAH, $C_6H_{13}NO_5 \cdot HCl$, CAS registry number: 66-84-2, Figure 1), a natural amino monosaccharide, is a marine biopreparation extracted from chitin [1]. Glucosamine hydrochloride is one of two commonly used salts, and the other is sulfate. Glucosamine is primarily a dietary additive. It is well known that the body's ability to synthesize glucosamine gradually declines with age. Intaking a certain amount of glucosamine hydrochloride can provide a supplement for the lack of glucosamine in the human body. However, whether it can prevent and relieve arthritis needs further research [2].

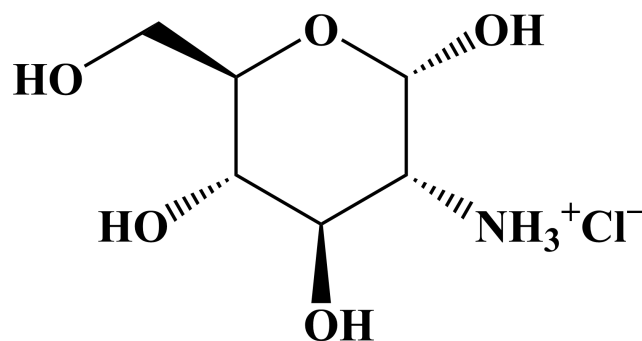


Figure 1. Molecular structure of GAH.

Solubility is one of the most basic in crystallization research. As a basic property of a substance, solubility can provide data for the selection of crystallization methods and processes [3]. There are two measuring methods for solubility: the static method and the dynamic method [4]. The dynamic method is suitable for substances that undergo polymorph transformation in solvents, while the static method is suitable for stable substances. Faiyaz Shakeel et al. determined the solubility of pterostilbene in some pure solvents and different cosolvent compositions by static method [5]. The solubility data can be used in purification, recrystallization, drug discovery, pre-formulation studies, and dosage form design, especially in the pharmaceutical, food, and nutritional health industries. Faiyaz Shakeel et al. also determined the solubility of gefitinib in organic solvents using the isothermal saturation shaker method, and the solubility data for measuring gefitinib is of great significance in various industrial processes such as its drug discovery process and formulation development [6].

When salt is used as an additive, it sometimes reduces the solubility of a substance and sometimes increases its solubility. For example, N. Mani et al. used salt and sugar as additives to reduce the solubility of guaifenesin [7]. The effect of acidity on solubility is also very obvious, for example, S. Mishra et al. found that the solubility of triisooamyl phosphate first decreased and then increased with the increase of acidity [8]. Crystallization is a key step in the separation and purification, and the factors that affect crystallization are often the influence of temperature, supersaturation, stirring rate, and additives, adding additives to the solution will cause a change in the solubility of the crystalline components, which mainly depends on the role of foreign ions and pH value [9].

GAH plays an important role in the human body [10]. Research on GAH is mostly focused on pharmacological effects, but few on its dissolution thermodynamics [11]. Our team has studied the solid-liquid equilibrium of GAH in four binary solvents, but the solubility data of GAH in the literature is still insufficient [12].

The aim of this work is to help guide the design of crystallization and obtain higher product yield by adding different additives to the pure water system. In this study, the solubility of GAH in the presence of additives (HCl, NaCl, and KCl) in the range of 283.15 K to 323.15 K was determined by gravimetry [13]. The modified Apelblat model and van't Hoff model were used to correlate the solubility data [14]. This work can provide an important reference for the crystallization and preparation of GAH. The effects of GAH on crystal morphology, particle size, and yield in the presence of HCl, NaCl, and KCl were studied by cooling crystallization, and the products were characterized by powder X-ray diffraction, polarizing microscopy, and crystal size analyzer [15].

2. Experimental Section

2.1. Materials

GAH is provided by Shanghai Macklin Biochemical Technology Co., Ltd. (Shanghai, China), with a mass fraction of purity greater than 0.99. The additives including HCl, NaCl, and KCl used in the experiment were purchased from Sinopharm Chemical Reagent Co., Ltd. (Shanghai, China) The deionized water used in the experiment was made by our laboratory using arium advance EDI, Sartorius, Germany, and all the chemicals were not further purified. The source and purity of the materials used in the experiment are shown in Table 1.

2.2. Powder X-ray Diffraction Measurement

The GAH crystals were identified by powder X-ray diffraction (PXRD) analysis on Mini Flex 600 (Rigaku Corporation of Japan, Akishima-shi, Japan) instrument, using Cu K α radiation (0.15405 nm). The tube voltage is 40 kV, and the current is 30 mA. PXRD data were collected at $2\theta = 5^{\circ}$ – 50° , with a step size of 0.02° and a scanning speed of 8° /min.

Table 1. Detailed information of the chemicals used in this work.

Materials	CAS Number	Source	Relative Molecular Mass	Mass Fraction Purity	Analysis Method
GAH	66-84-2	Shanghai Macklin Biochemical Technology Co., Ltd.	215.63	≥0.990	HPLC ^a
Hydrochloric acid	7647-01-0	Sinopharm Chemical Reagent Co., Ltd., China	36.50	0.360–0.380	HPLC ^a
NaCl	7647-14-5	Sinopharm Chemical Reagent Co., Ltd., China	58.50	≥0.995	HPLC ^a
KCl	7447-40-7	Sinopharm Chemical Reagent Co., Ltd., China	74.50	≥0.995	HPLC ^a

^a High-performance liquid chromatography.

2.3. Infrared Spectroscopy Measurement

Infrared (IR) spectra of GAH crystals were recorded with Vertex 70 IR spectrometer (Germany). Measurements were made using KBr particles in the range of 4000 cm⁻¹ to 500 cm⁻¹, with a resolution of 4 cm⁻¹.

2.4. Solubility Measurements

In the temperature range of 278.15 K to 318.15 K, the solubility data of GAH in pure water in the absence and presence of three additives were determined by gravimetry [16,17]. 20 g of water was added to the glass bottle, after which a sufficient amount of GAH solids was added to the glass bottle, and different kinds of additives were added to the glass bottle. Bottles were placed in double-jacketed glass containers filled with water at a temperature controlled by a thermostatic bath (CF 41, Julabo, Germany; Accuracy ± 0.05 K). Preliminary experiments were carried out in all the experimental solvents, the lowest temperature was 278.15 K, and the highest temperature was 323.15 K. In order to achieve solid-liquid equilibrium, the suspension is magnetically stirred at constant temperature for at least 12 h and then precipitated without agitation for 4 h. About 5 mL of the supernatant was filtered from the glass bottle using a membrane with a diameter of 0.45 μm using a pre-cooled or preheated syringe into a pre-weighed weighing bottle. The total mass of the weighing bottle and solution was immediately weighed. The sample was first dried in a fume hood and then dried in a vacuum oven at 318.15 K for more than 15 h. The weight of the bottle was measured several times until the weight was constant, indicating that drying was complete. All masses were measured using an electronic balance (Model ME, Mettler Toledo, Greifensee, Switzerland) with an accuracy of ±0.0001 g. Each solubility measurement was repeated three times to calculate the arithmetic mean. The mole fraction solubility [18] of GAH in the presence of additive is calculated from Equation (1):

$$x_1 = \frac{m_1/M_1}{m_1/M_1 + m_2/M_2 + m_3/M_3} \quad (1)$$

where m_1 , m_2 , and m_3 stand for the masses of GAH, water, and additives (HCl, NaCl, and KCl), respectively. Correspondingly, the terms M_1 , M_2 , and M_3 represent their molecular weight.

2.5. The Cooling Crystallization of GAH with the Presence of Additives

The solution was prepared according to the saturation solubility measured at 323.15 K. 80 g pure water was accurately weighed, and 41.6 g GAH was added to the glass bottles. The temperature control was ensured by the Huber editable circulator. The initial temperature was set at 328.15 K, and the stirring rate was 160 rpm. After the solute was completely dissolved, additives (mole concentrations were HCl: 0.0356, 0.00049, 0.00025, 0.0090, 0.0323; NaCl: 0.0091, 0.0356, 0.0580; KCl: 0.0099, 0.0385, and 0.0570) were added to the glass bottles. The crystallization temperature was reduced to the final temperature of 288.15 K

with a cooling rate of 0.2 K/min. The crystal morphology was observed by the polarizing microscopy (BX53M, Olympus Corporation, Tokyo, Japan). The constant temperature water bath and stirring were closed at the same time, and the slurry in the crystallizer was transferred to the Brinell funnel for filtration. The product was dried in a vacuum drying oven, and the dried product was weighed. The particle size of the product was analyzed by a crystal size analyzer (MASTERSIZER3000, Malvern Instruments Limited, Malvern, UK).

3. Thermodynamic Models

3.1. Modified Apelblat Model

The modified Apelblat [19,20] equation is a semi-empirical equation with high precision. The solubility of GAH with different temperatures is fitted by using this semi-empirical model. The Apelblat equation is expressed by Equation (2) [21]:

$$\ln x_1 = A + \frac{B}{T} + C \ln T \quad (2)$$

where x_1 is the mole fraction solubility of GAH; T is the absolute temperature; A , B , and C are represented as the three parameters of the model. A and B represent the change in the activity coefficient of the solution, and C represents the effect of temperature on the enthalpy of fusion.

3.2. Van't Hoff Model

The van't Hoff model [22,23] describes the linear relationship between the logarithm of the molar fraction solubility and the reciprocal absolute temperature. It can be described as Equation (3) [24]:

$$\ln x_1 = \frac{-\Delta H_d}{RT} + \frac{\Delta S_d}{R} \quad (3)$$

where x_1 is the mole fraction solubility of the GAH, T is the temperature (K), ΔH_d is the ideal enthalpy of solution, ΔS_d is the ideal entropy of solution, and R is the ideal gas constant, respectively. $-\frac{\Delta H_d}{R}$ and $\frac{\Delta S_d}{R}$ can be abbreviated as B and A since they are fixed values. Therefore, we rearrange Equation (3) into Equation (4):

$$\ln x_1 = A + \frac{B}{T} \quad (4)$$

where A represents the $\Delta S_d/R$; B represents the $-\Delta H_d/R$.

The relative average deviation (ARD) [25] and root mean square deviation (RMSD) [26] were calculated to verify the accuracy of the correlated data. x_i^{exp} and x_i^{cal} are the experimental and calculated solubility data, respectively. n denotes the number of experimental points. The expression is as follows [24,27].

$$ARD\% = \frac{100}{n} \sum_{i=1}^n \left| \frac{x_i^{exp} - x_i^{cal}}{x_i^{exp}} \right| \quad (5)$$

$$RMSD = \sqrt{\frac{\sum_{i=1}^n (x_i^{cal} - x_i^{exp})^2}{n}} \quad (6)$$

4. Results and Discussion

4.1. PXRD Analysis

GAH and solid phase residues were characterized by PXRD. As shown in Figure 2, Since some solution was left in the solid phase during filtration, a small amount of NaCl and KCl would be precipitated. It showed that the peak position of GAH was similar [12], and the diffraction peak of the KCl system appeared at 28.14° (which is circled in red), but its peak intensity was small. The main peak of NaCl coincided with the peak of GAH at 31.46° (which is circled in red), resulting in a stronger peak strength of 31.46° than that of a

pure water system. Therefore, GAH is stable in aqueous solution and does not undergo polymorph transformation.

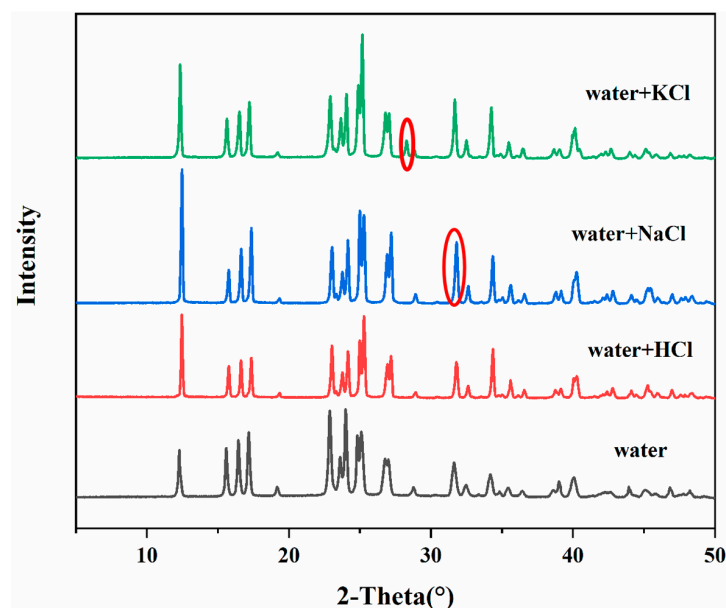


Figure 2. The PXRD pattern of raw GAH and solid phase insoluble in water phase.

4.2. Infrared Spectroscopic Analysis

GAH and solid phase residues containing different additives (HCl, NaCl, and KCl) were characterized by infrared spectroscopy (Figure 3). When the organic molecules are irradiated with infrared light, the chemical bonds or functional groups in the molecules can be vibrationally absorbed. As can be seen from the atlas, the positions of peaks are consistent, indicating that GAH has not undergone chemical changes.

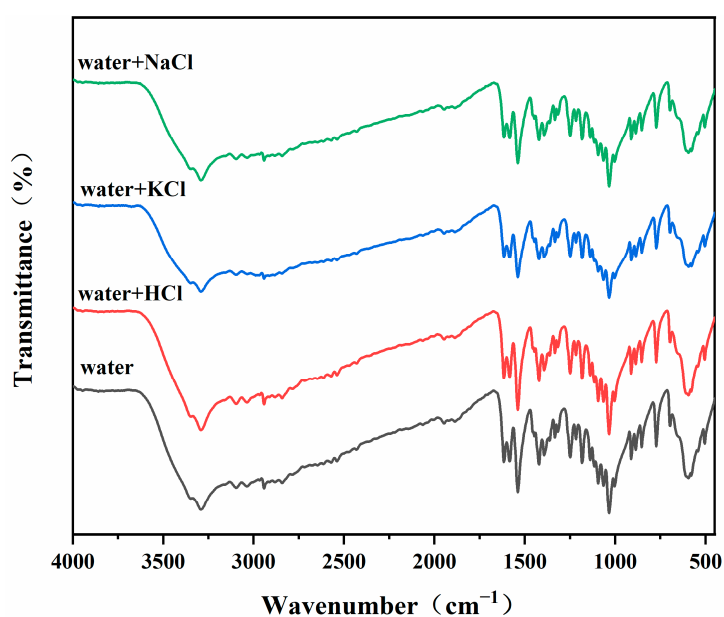


Figure 3. GAH infrared spectra with different additives (HCl, NaCl, and KCl).

4.3. Experimental Solubility Data

The solubility of GAH in pure water has been reported in the literature [12]. The relative error of the solubility data between the literature and this work is less than 3.5%, which might be caused by differences in raw material resources. In addition to water, this

study has also determined the solubility of GAH in the presence of acid or salts. This meets the environment of industrial crystallization and helps to guide the practical production of GAH crystals. All the solubility data of this experiment are summarized in Tables 2–4, and the solubility curve is drawn in Figures S1–S3. At the same temperature and with almost the same molar concentration of the additive, the solubility of GAH is the lowest when HCl is used as an additive, the solubility of GAH is the second when NaCl is used as an additive, and the solubility of KCl is higher than that of HCl and NaCl systems.

Table 2. Experimental and calculated mole fraction solubility of GAH from 278.15 K to 318.15 K in water when HCl was used as an additive ($p = 0.1$ Mpa) ^{a,b}.

x_{HCl}	$10^3 x_1^{\text{exp}}$	$10^3 x_1^{\text{Apelblat}}$	$10^3 x_1^{\text{van't}}$
		278.15 K	
0.0000	21.65	21.64	21.64
0.0023	19.80	19.79	19.79
0.0046	18.54	18.58	18.58
0.0090	15.99	15.96	15.96
0.0173	12.35	12.15	12.15
0.0251	9.659	9.509	9.509
0.0323	7.766	7.504	7.504
0.0453	5.488	5.118	5.118
		283.15 K	
0.0000	23.38	23.39	23.28
0.0023	21.50	21.51	21.42
0.0046	20.29	20.25	20.17
0.0090	17.55	17.58	17.55
0.0173	13.31	13.61	13.62
0.0251	10.72	10.71	10.69
0.0323	8.217	8.491	8.416
0.0453	5.415	5.742	5.596
		288.15 K	
0.0000	25.16	25.25	25.25
0.0023	23.40	23.33	23.33
0.0046	22.10	22.03	22.03
0.0090	19.47	19.32	19.32
0.0173	15.09	15.19	15.20
0.0251	11.71	12.03	12.04
0.0323	9.321	9.593	9.593
0.0453	6.150	6.465	6.457
		293.15 K	
0.0000	27.40	27.22	27.30
0.0023	25.10	25.27	25.33
0.0046	23.85	23.93	23.99
0.0090	20.79	21.17	21.21
0.0173	17.18	16.89	16.90
0.0251	13.23	13.47	13.51
0.0323	11.02	10.82	10.89
0.0453	7.501	7.300	7.415
		298.15 K	
0.0000	29.22	29.31	29.45
0.0023	27.39	27.33	27.43
0.0046	26.01	25.94	26.04
0.0090	23.33	23.15	23.20
0.0173	18.62	18.71	18.72
0.0251	15.25	15.04	15.1
0.0323	12.16	12.19	12.30
0.0453	8.221	8.268	8.475

Table 2. *Cont.*

x_{HCl}	$10^3 x_1^{\text{exp}}$	$10^3 x_1^{\text{Apelblat}}$	$10^3 x_1^{\text{van't}}$
303.15 K			
0.0000	31.46	31.53	31.69
0.0023	29.58	29.51	29.63
0.0046	28.11	28.08	28.20
0.0090	25.33	25.25	25.31
0.0173	20.75	20.66	20.67
0.0251	17.02	16.75	16.82
0.0323	14.13	13.71	13.84
0.0453	9.826	9.387	9.643
308.15 K			
0.0000	33.92	33.88	34.02
0.0023	31.93	31.82	31.92
0.0046	30.04	30.35	30.46
0.0090	27.48	27.48	27.53
0.0173	22.67	22.74	22.75
0.0251	18.78	18.61	18.67
0.0323	15.39	15.39	15.52
0.0453	10.78	10.68	10.93
313.15 K			
0.0000	36.37	36.36	36.43
0.0023	34.08	34.25	34.31
0.0046	32.83	32.75	32.81
0.0090	29.84	29.84	29.87
0.0173	25.04	24.96	24.97
0.0251	20.63	20.62	20.65
0.0323	17.11	17.26	17.34
0.0453	12.25	12.18	12.33
318.15 K			
0.0000	39.08	38.98	38.93
0.0023	36.86	36.82	36.79
0.0046	35.68	35.29	35.27
0.0090	32.45	32.34	32.32
0.0173	27.39	27.32	27.31
0.0251	22.78	22.80	22.77
0.0323	19.36	19.33	19.30
0.0453	13.76	13.92	13.87
323.15 K			
0.0000	41.66	41.74	41.52
0.0023	39.54	39.54	39.37
0.0046	37.77	37.98	37.82
0.0090	34.86	34.98	34.89
0.0173	29.70	29.82	29.80
0.0251	24.96	25.16	25.03
0.0323	21.51	21.62	21.41
0.0453	15.77	15.94	15.54

^a x_1^{exp} is the experimental solubility of GAH x_1^{Apelblat} and $x_1^{\text{van't Hoff}}$ are the solubility calculated by the modified Apelbalt model and van't Hoff model, respectively. x_{HCl} represents the mole fraction of HCl in a pure water system. ^b The standard uncertainty is $u(T) = 0.05$ K. The relative standard uncertainty u_r is $u_r(x_1) = 0.05$, $u_r(x_2) = 0.001$.

Table 3. Experimental and calculated mole fraction solubility of GAH from 278.15 K to 318.15 K in water when NaCl is used as an additive ($p = 0.1$ Mpa) ^{a,b}.

x_{NaCl}	$10^3 x_1^{\text{exp}}$	$10^3 x_1^{\text{Apelblat}}$	$10^3 x_1^{\text{van't}}$
278.15 K			
0.0000	21.65	21.64	21.40
0.0091	17.89	17.79	17.44
0.0181	14.02	14.05	13.98

Table 3. Cont.

x_{NaCl}	$10^3 x_1^{exp}$		$10^3 x_1^{Apelblat}$	$10^3 x_1^{van't}$
0.0356	8.708		8.891	9.164
0.0441	7.146		7.310	7.509
0.0580	5.376		5.526	5.617
0.0845	4.047		4.097	3.860
		283.15 K		
0.0000	23.38		23.39	23.28
0.0091	19.32		19.32	19.15
0.0181	15.60		15.56	15.52
0.0356	10.45		10.23	10.38
0.0441	8.568		8.460	8.573
0.0580	6.518		6.404	6.453
0.0845	4.466		4.528	4.396
		288.15 K		
0.0000	25.16		25.25	25.25
0.0091	20.86		20.96	20.96
0.0181	17.27		17.19	17.18
0.0356	11.85		11.67	11.70
0.0441	10.10		9.714	9.743
0.0580	7.718		7.370	7.379
0.0845	5.226		5.018	4.984
		293.15 K		
0.0000	27.40		27.22	27.30
0.0091	22.56		22.75	22.87
0.0181	18.85		18.93	18.95
0.0356	13.26		13.21	13.14
0.0441	11.17		11.07	11.02
0.0580	8.372		8.426	8.398
0.0845	5.719		5.576	5.627
		298.15 K		
0.0000	29.22		29.31	29.45
0.0091	24.66		24.67	24.88
0.0181	20.70		20.79	20.84
0.0356	14.74		14.84	14.69
0.0441	12.18		12.52	12.42
0.0580	9.450		9.571	9.517
0.0845	6.166		6.211	6.327
		303.15 K		
0.0000	31.46		31.53	31.69
0.0091	26.78		26.75	27.00
0.0181	22.76		22.79	22.83
0.0356	16.33		16.56	16.37
0.0441	13.83		14.07	13.94
0.0580	10.65		10.81	10.74
0.0845	6.714		6.933	7.086
		308.15 K		
0.0000	33.92		33.88	34.02
0.0091	29.23		28.99	29.21
0.0181	25.07		24.91	24.95
0.0356	18.26		18.36	18.18
0.0441	15.75		15.72	15.59
0.0580	12.13		12.14	12.07
0.0845	7.666		7.754	7.907
		313.15 K		
0.0000	36.37		36.36	36.43
0.0091	31.54		31.41	31.53
0.0181	27.18		27.16	27.19
0.0356	20.29		20.22	20.12
0.0441	17.56		17.45	17.37

Table 3. *Cont.*

x_{NaCl}	$10^3 x_1^{\text{exp}}$	$10^3 x_1^{\text{Apelblat}}$	$10^3 x_1^{\text{van't}}$
0.0580	13.46	13.55	13.52
0.0845	8.812	8.687	8.793
318.15 K			
0.0000	39.08	38.98	38.93
0.0091	34.11	34.02	33.95
0.0181	29.45	29.55	29.54
0.0356	22.17	22.15	22.20
0.0441	19.29	19.25	19.29
0.0580	15.07	15.06	15.09
0.0845	9.664	9.748	9.745
323.15 K			
0.0000	41.66	41.74	41.52
0.0091	36.56	36.83	36.47
0.0181	32.11	32.09	32.02
0.0356	24.23	24.13	24.41
0.0441	21.19	21.14	21.35
0.0580	16.84	16.66	16.79
0.0845	11.08	10.95	10.77

^a x_1^{exp} is the experimental solubility of GAH x_1^{Apelblat} and $x_1^{\text{van't Hoff}}$ are the solubility calculated by the modified Apelblat model and van't Hoff model, respectively. x_{NaCl} represents the mole fraction of NaCl in a pure water system. ^b The standard uncertainty is $u(T) = 0.05$ K. The relative standard uncertainty u_r is $u_r(x_1) = 0.05$, $u_r(x_2) = 0.001$.

Table 4. Experimental and calculated mole fraction solubility of GAH from 278.15 K to 318.15 K in water when KCl is used as an additive ($p = 0.1$ Mpa) ^{a,b}.

x_{KCl}	$10^3 x_1^{\text{exp}}$	$10^3 x_1^{\text{Apelblat}}$	$10^3 x_1^{\text{van't}}$
278.15 K			
0.0000	21.65	21.64	21.4
0.0099	17.83	17.98	18.02
0.0196	15.35	15.49	15.34
0.0385	11.87	11.64	11.40
0.0477	9.852	9.804	9.873
0.0570	7.864	7.945	8.399
0.0741	4.765	4.997	5.994
283.15 K			
0.0000	23.38	23.39	23.28
0.0099	19.81	19.74	19.76
0.0196	17.23	17.02	16.94
0.0385	12.72	12.85	12.74
0.0477	11.17	11.08	11.12
0.0570	9.403	9.286	9.543
0.0741	6.638	6.362	6.985
288.15 K			
0.0000	25.16	25.25	25.25
0.0099	21.91	21.60	21.60
0.0196	18.74	18.66	18.65
0.0385	14.01	14.17	14.17
0.0477	12.36	12.45	12.48
0.0570	10.77	10.73	10.79
0.0741	8.058	7.883	8.096
293.15 K			
0.0000	27.40	27.22	27.30
0.0099	23.59	23.56	23.54
0.0196	20.41	20.42	20.47
0.0385	15.38	15.61	15.71

Table 4. Cont.

x_{KCl}	$10^3 x_1^{exp}$	$10^3 x_1^{Apelblat}$	$10^3 x_1^{van't}$
0.0477	13.72	13.94	13.95
0.0570	12.34	12.27	12.16
0.0741	9.809	9.524	9.337
298.15 K			
0.0000	29.22	29.31	29.45
0.0099	25.49	25.61	25.58
0.0196	22.14	22.30	22.39
0.0385	17.14	17.19	17.36
0.0477	15.43	15.54	15.53
0.0570	13.78	13.88	13.64
0.0741	11.52	11.24	10.72
303.15 K			
0.0000	31.46	31.53	31.69
0.0099	27.56	27.76	27.73
0.0196	24.25	24.31	24.42
0.0385	18.91	18.92	19.12
0.0477	17.23	17.25	17.23
0.0570	15.38	15.56	15.25
0.0741	12.66	12.97	12.24
308.15 K			
0.0000	33.92	33.88	34.02
0.0099	29.97	29.99	29.97
0.0196	26.53	26.46	26.56
0.0385	21.14	20.81	20.99
0.0477	19.46	19.08	19.05
0.0570	17.34	17.28	16.98
0.0741	14.01	14.66	13.93
313.15 K			
0.0000	36.37	36.36	36.43
0.0099	32.31	32.32	32.31
0.0196	28.73	28.75	28.81
0.0385	23.37	22.87	22.97
0.0477	21.24	21.02	21.00
0.0570	19.19	19.03	18.85
0.0741	15.79	16.24	15.78
318.15 K			
0.0000	39.08	38.98	38.93
0.0099	34.73	34.74	34.76
0.0196	31.22	31.19	31.17
0.0385	25.33	25.12	25.07
0.0477	23.24	23.08	23.08
0.0570	20.64	20.79	20.85
0.0741	17.85	17.67	17.81
323.15 K			
0.0000	41.66	41.74	41.52
0.0099	37.38	37.25	37.30
0.0196	33.79	33.78	33.64
0.0385	26.95	27.58	27.28
0.0477	24.86	25.26	25.28
0.0570	22.63	22.55	22.99
0.0741	19.53	18.89	20.02

^a x_1^{exp} is the experimental solubility of GAH $x_1^{Apelblat}$ and $x_1^{van't Hoff}$ are the solubility calculated by the modified Apelbalt model and van't Hoff model, respectively. The x_{KCl} represents the mole fraction of KCl in a pure water system. ^b The standard uncertainty is $u(T) = 0.05$ K. The relative standard uncertainty u_r is $u_r(x_1) = 0.05$, $u_r(x_2) = 0.001$.

As can be seen from the solubility diagram above, the solubility value of GAH increases with the increase in temperature. When the temperature increases, the thermal movement

of molecules is intensified, and the collision frequency between solute molecules and solvent molecules is increased, which is manifested as the increase of GAH solubility on the macro level. At the same absolute temperature, the solubility of GAH decreases with the increase of additive concentration.

The factors that affect the solubility of GAH in the presence of different additives might be different. In the presence of NaCl and KCl, the pH value of the solution system does not change, and the solubility of GAH gradually decreases with the addition of additives. At this time, the main effect affecting the solubility of GAH is the isoionic effect. Strong electrolytes NaCl and KCl ionize the same chloride ions carried by GAH, resulting in reduced solubility of GAH. In order to further study whether chloride ions affect solubility, the experiment of hydrochloric acid was designed. In the presence of HCl, the pH in the solution will decrease [28]. In general, drugs can be divided into two categories according to the effect of pH: the solubility of one class of drugs increases with the decrease of pH, and the solubility of the other class of drugs decreases with the decrease of pH [29]. It can be seen that GAH belongs to the latter class of drugs. After the addition of HCl, HCl contains chloride ions and hydrogen ions. These two actions worked together to make the decline in solubility even more pronounced. In addition, when HCl, NaCl, and KCl are used as additives, chloride ions are the same, hydrogen ions have the smallest ionic radius, and sodium ions have a smaller ionic radius than potassium ions. It can be seen that the solubility of GAH increases with the increase of the ionic radius of the cation in the additives.

4.4. Data Correlation

The modified Apelblat model and van't Hoff thermodynamic model were used for correlation analysis. In general, the smaller the ARD value, the better the fitting result. The parameters of the modified Apelblat model and van't Hoff model, ARD, and RMSD of the GAH are shown in Tables S1–S6 in the Supporting Information. By calculating and comparing the average of ARD, we estimated the correlation accuracy of the thermodynamic models. The van't Hoff model and the Modified Apelblat model can predict the solubility data at different temperatures, and the above models have good fitting effects [30]. The ARD values of the Modified Apelblat model are smaller than those of the van't Hoff model. Therefore, the fitting trend lines using the modified Apelblat model were added to the solubility diagrams in Figures S1–S3, which show a good fitting effect and verify the accuracy of the data [31].

Moreover, the calculated parameters of the van't Hoff model shown in Tables S4–S6 can be considered as the ideal thermodynamic dissolution properties. It can be found that the values of ΔH_d and ΔS_d are all positive in the experimental solutions, indicating that the dissolution processes of GAH in this work are all endothermic and entropy-driven.

4.5. Effects of Additive on GAH Crystal Morphology

The morphology and particle size of the crystal product are often changed by the solution composition and operation conditions of the crystallization process [32]. In this work, cooling crystallization experiments of GAH were carried out under different conditions, especially the effects of different additives (HCl, NaCl, and KCl) on the morphology, particle size, and yield of GAH crystals were studied [33].

The crystal morphology obtained by cooling crystallization is shown in Figure 4. When there was no additive, most of the crystals of GAH cooled in pure water were polyhedral. When a lower concentration of HCl (mole concentration 0.00025) was added to the pure water system, GAH presented a regular cubic shape. When HCl with a mole concentration of 0.00049 was added to the pure water system, the GAH also exhibited a regular cubic shape. It can be seen that when higher concentrations of HCl (0.0023, 0.0090, and 0.0323) were used as the additive, the crystal morphology was mostly trihedral. With the increase of HCl concentration, the crystal morphology of GAH tended to be polyhedral. When NaCl (mole concentration 0.0091, 0.0356, and 0.0580) was used as additives, the crystal

morphology was mostly tetrahedral, while when KCl (mole concentration 0.0099, 0.0385, and 0.0323) was used as additives, the crystal morphology tended to be bipyramidal [34].

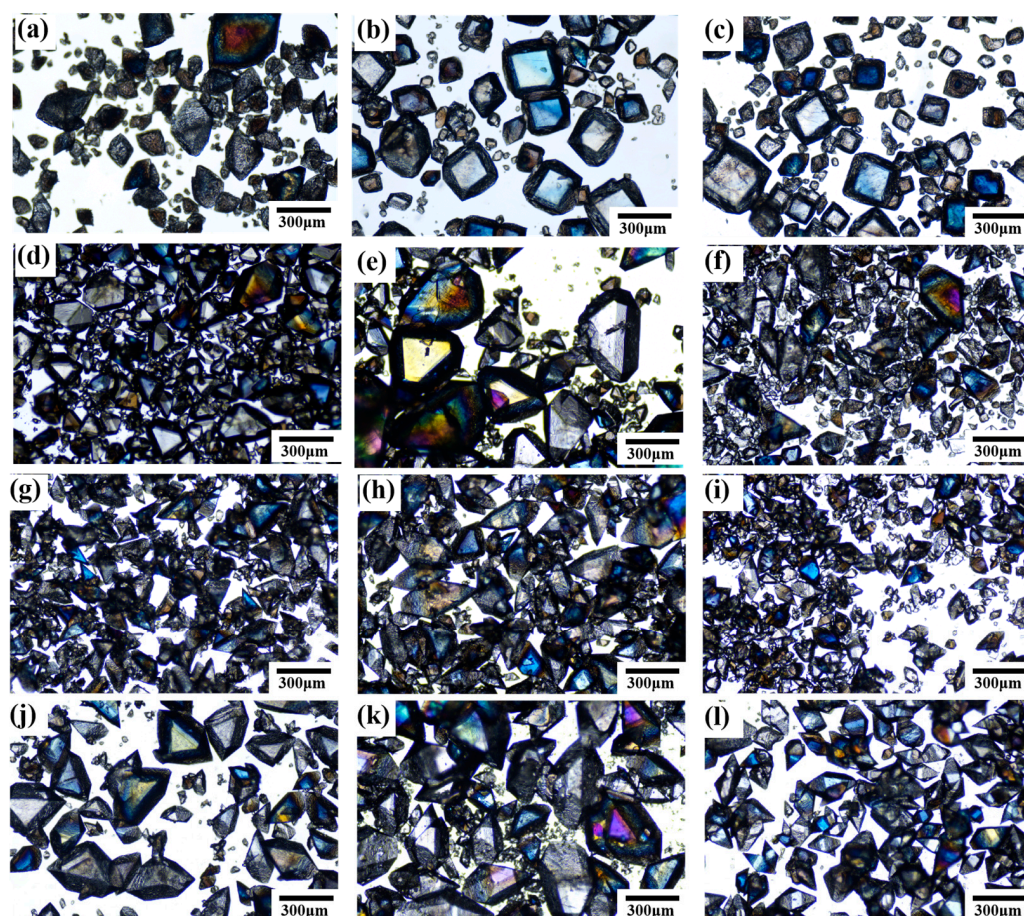


Figure 4. Microscopic images of GAH crystals obtained at different concentrations of additives: (a) water, (b) HCl, 0.00025, (c) HCl, 0.00049, (d) HCl, 0.0023, (e) HCl, 0.0090, (f) HCl, 0.0323, (g) NaCl, 0.0091, (h) NaCl, 0.0356, (i) NaCl, 0.0580, (j) KCl, 0.0099, (k) KCl, 0.0385, and (l) KCl 0.0570.

It can be seen from the particle size distribution diagram (Figure 5a) that the average size D50 of GAH in pure water is 369 μm , and the D50 of GAH when HCl was used as an additive is 221 μm . When NaCl was used as an additive, the D50 of GAH was 297 μm . It can be seen that the particle size of GAH at this time is smaller than that of GAH in the pure water system. While KCl was used as an additives, the D50 of GAH is 357 μm . The particle size is similar to that of the pure water system.

From the yield histogram (Figure 5b), when there was no additive in GAH, the theoretical yield was 40.54% and the actual yield was 36.37%. When HCl with a mole concentration of 0.0323 was used as the additive, the theoretical yield was 71.39%, when NaCl with a mole concentration of 0.035 was used as the additive, the theoretical yield was 71.36%, and the actual yield was 69.46%. When KCl with a mole concentration of 0.057 was used as an additive, the theoretical yield was 73.4% and the actual yield was 66.95%. It could be seen that the above additives can greatly increase the yield of GAH crystal products. At the same mole concentration, when HCl was additive, the yield was the highest, followed by NaCl, and the lowest when KCl was the additive. However, the effects of additives at higher concentrations are not explored in this work since salt would precipitate during the crystallization process of GAH.

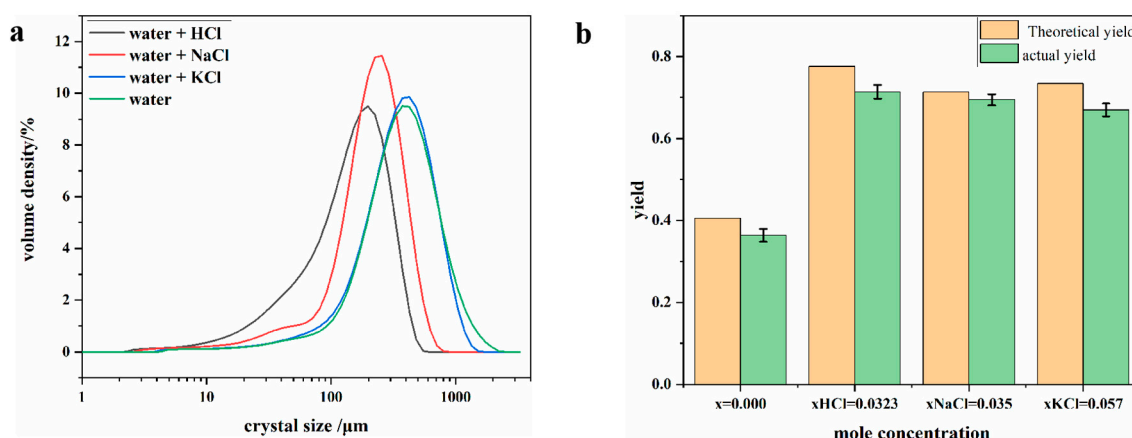


Figure 5. Particle size distribution and yield of GAH crystallized from different aqueous solutions: (a), particle size distribution of GAH; (b), theoretical and actual yield of GAH.

5. Conclusions

In this study, the solubility of GAH in the presence of additives (HCl, NaCl, and KCl) at temperatures ranging from 278.15 K to 323.15 K was measured by gravimetric method. At the same temperature and similar additive concentration, HCl had the greatest effect on the solubility of GAH, followed by NaCl and KCl. The modified Apelblat model and van't Hoff model were used to well correlate the solubility data. The cooling crystallization process of GAH was carried out in the presence of additives, showing that the three additives have an influence on the morphology of GAH. When low-concentration HCl was used, the crystal morphology of GAH was cubic. As the concentration of HCl increased, the crystal morphology of GAH was close to the tetrahedron. In the presence of NaCl, the crystal morphology is mostly tetrahedral. When KCl was used as an additive, the crystal morphology evolved to be bipyramidal and GAH had the largest particle size. The yield of cooling crystallization with additives was much higher than that of pure water systems. Under the same additive concentration, the yield was the maximum when HCl was added. This work can help design the crystallization process by adding the additives to obtain a high yield of glucosamine hydrochloride from an aqueous system instead of adding many organic solvents.

Supplementary Materials: The following supporting information can be downloaded at: <https://www.mdpi.com/article/10.3390/cryst13091326/s1>, Figure S1. Mole fraction solubility of GAH in water with different HCl concentrations at the temperature range of 278.15–323.15 K. Figure S2. Mole fraction solubility of GAH in water with different NaCl concentrations at the temperature range of 278.15–323.15 K. Figure S3. Mole fraction solubility of GAH in water with different KCl concentrations at the temperature range of 278.15–323.15 K. Table S1: The parameters of the modified Apelblat equation when HCl was used as an additive. Table S2: The parameters of the modified Apelblat equation when NaCl was used as an additive. Table S3: The parameters of the modified Apelblat equation when KCl was used as an additive. Table S4: The parameters of the van't Hoff equation when HCl was used as an additive. Table S5: The parameters of the van't Hoff equation when NaCl was used as additive. Table S6: The parameters of the van't Hoff equation when KCl was used as additive.

Author Contributions: Conceptualization, Z.P. and S.D.; methodology, Z.P.; formal analysis, Q.Z., J.T. and Y.X.; investigation, Z.P., J.T. and Y.X.; resources, J.L. and Q.Z.; software, Z.P. and Y.W.; writing—original draft, Z.P. and Y.W.; writing—review and editing, S.D. and Y.W.; supervision, F.X. and S.D.; funding acquisition, S.D., F.X. and Y.W. All authors have read and agreed to the published version of the manuscript.

Funding: This research was funded by the Key R&D Program of Shandong Province, China (2021CXGC010811), National Natural Science Foundation of China (NNSFC 22008175), Shandong Provincial Natural Science Foundation (ZR2023MB036), Central Guidance on Local Science and

Technology Development Fund of Shandong Province (YDZX2021054), Jinan Introducing Innovation Team Project (202228033), Science, Education and Industry Integration Technology Innovation Project (2022PY065) and the Talent Research Project of Qilu University of Technology (2023RCKY076).

Data Availability Statement: The data presented in this study are available in this article and the Supplementary Materials.

Conflicts of Interest: The authors declare no conflict of interest.

References

1. Tamai, Y.; Miyatake, K.; Okamoto, Y.; Takamori, Y.; Sakamoto, H.; Minami, S. Enhanced healing of cartilaginous injuries by glucosamine hydrochloride. *Carbohydr. Polym.* **2002**, *48*, 369–378. [[CrossRef](#)]
2. Jamialahmadi, K.; Arasteh, O.; Matbou Riahi, M.; Mehri, S.; Riahi-Zanjani, B.; Karimi, G. Protective effects of glucosamine hydrochloride against free radical-induced erythrocytes damage. *Environ. Toxicol. Pharmacol.* **2014**, *38*, 212–219. [[CrossRef](#)] [[PubMed](#)]
3. Huang, Z.; Sha, J.; Chang, Y.; Cao, Z.; Hu, X.; Li, Y.; Li, T.; Ren, B. Solubility measurement, model evaluation and Hansen solubility parameter of ipriflavone in three binary solvents. *J. Chem. Thermodyn.* **2021**, *152*, 106285. [[CrossRef](#)]
4. Sang, J.; Wang, H.; Jin, J.; Meng, H. Comparison and modelling of rutin solubility in supercritical carbon dioxide and subcritical 1,1,1,2-tetrafluoroethane. *J. CO₂ Util.* **2017**, *21*, 1–8. [[CrossRef](#)]
5. Alshehri, S.; Shakeel, F. Solubility determination, various solubility parameters and solution thermodynamics of sunitinib malate in some cosolvents, water and various (Transcutol + water) mixtures. *J. Mol. Liq.* **2020**, *307*, 112970. [[CrossRef](#)]
6. Alanazi, A.; Alshehri, S.; Altamimi, M.; Shakeel, F. Solubility determination and three dimensional Hansen solubility parameters of gefitinib in different organic solvents: Experimental and computational approaches. *J. Mol. Liq.* **2020**, *299*, 112211. [[CrossRef](#)]
7. Mani, N.; Jun, H.W.; Beach, J.W.; Nerurkar, J. Solubility of Guaifenesin in the Presence of Common Pharmaceutical Additives. *Pharm. Dev. Technol.* **2003**, *8*, 385–396. [[CrossRef](#)] [[PubMed](#)]
8. Mishra, S.; Kumar, M.; Pandey, N.K. Aqueous solubility of tri-iso-amyl phosphate (TiAP)—Effect of acidity, temperature and metal ions. *Prog. Nucl. Energy* **2020**, *119*, 103166. [[CrossRef](#)]
9. Hrkovac, M.; Kardum, J.P.; Ukrainczyk, N. Influence of NaCl on Granulometric Characteristics and Polymorphism in Batch-Cooling Crystallization of Glycine. *Chem. Eng. Technol.* **2015**, *38*, 139–146. [[CrossRef](#)]
10. Jeong, D.-H.; Ullah, H.M.A.; Goo, M.-J.; Ghim, S.-G.; Hong, I.-H.; Kim, A.-Y.; Jeon, S.-M.; Choi, M.-S.; Elfadl, A.K.; Chung, M.-J.; et al. Effects of oral glucosamine hydrochloride and mucopolysaccharide protein in a rabbit model of osteoarthritis. *Int. J. Rheum. Dis.* **2018**, *21*, 620–628. [[CrossRef](#)]
11. Xing, R.; Liu, S.; Guo, Z.; Yu, H.; Li, C.; Ji, X.; Feng, J.; Li, P. The antioxidant activity of glucosamine hydrochloride in vitro. *Bioorg. Med. Chem.* **2006**, *14*, 1706–1709. [[CrossRef](#)]
12. Du, S.; Pan, Z.; Yu, C.; Lu, J.; Zhang, Q.; Gong, J.; Wang, Y.; Xue, F. Solid-liquid equilibrium of glucosamine hydrochloride in four binary solvents: Experiments, modeling, and molecular simulation. *J. Mol. Liq.* **2023**, *386*, 122564. [[CrossRef](#)]
13. Barzegar-Jalali, M.; Jafari, P.; Jouyban, A. Determination and correlation of naproxen solubility in polyethylene glycol dimethyl ether 250 and water mixtures. *Phys. Chem. Liq.* **2022**, *60*, 856–870. [[CrossRef](#)]
14. Jia, S.; Gao, Y.; Li, Z.; Zhang, T.; Liu, J.; Wang, J.; Gao, Z.; Gong, J. Process intensification and control strategies in cooling crystallization: Crystal size and morphology optimization of α -PABA. *Chem. Eng. Res. Des.* **2022**, *179*, 265–276. [[CrossRef](#)]
15. Liszi, I.; Blickle, T.; Liszi, J. Homogeneous nucleation in cooling crystallization. *Cryst. Res. Technol.* **1985**, *20*, 1309–1315. [[CrossRef](#)]
16. Kalam, M.A.; Alshamsan, A.; Alkholief, M.; Alsarra, I.A.; Ali, R.; Haq, N.; Anwer, M.K.; Shakeel, F. Solubility Measurement and Various Solubility Parameters of Glipizide in Different Neat Solvents. *ACS Omega* **2020**, *5*, 1708–1716. [[CrossRef](#)]
17. Hussain, A.; Altamimi, M.A.; Alshehri, S.; Imam, S.S. Assessment of solubility and Hansen solubility parameters of rifampicin in various permeation enhancers: Experimental and computational approach. *J. Mol. Liq.* **2021**, *328*, 115432. [[CrossRef](#)]
18. Yu, S.; Cheng, Y.; Xing, W.; Xue, F. Solubility determination and thermodynamic modelling of gliclazide in five binary solvent mixtures. *J. Mol. Liq.* **2020**, *311*, 113258. [[CrossRef](#)]
19. Ji, W.; Meng, Q.; Li, P.; Yang, B.; Wang, F.; Ding, L.; Wang, B. Measurement and Correlation of the Solubility of p-Coumaric Acid in Nine Pure and Water + Ethanol Mixed Solvents at Temperatures from 293.15 to 333.15 K. *J. Chem. Eng. Data* **2016**, *61*, 3457–3465. [[CrossRef](#)]
20. Alshehri, S.; Shakeel, F.; Alam, P.; Peña, Á.; Jouyban, A.; Martinez, F. Effect of temperature and polarity on the solubility and preferential solvation of sinapic acid in aqueous mixtures of DMSO and Carbitol. *J. Mol. Liq.* **2021**, *340*, 117268. [[CrossRef](#)]
21. Li, Z.; Zhang, T.; Huang, C.; Wang, H.; Yu, B.; Gong, J. Measurement and Correlation of the Solubility of Maltitol in Different Pure Solvents, Methanol–Water Mixtures, and Ethanol–Water Mixtures. *J. Chem. Eng. Data* **2016**, *61*, 1065–1070. [[CrossRef](#)]
22. Lan, G.; Li, X.; Chao, H.; Wang, N.; Wei, C.; Li, Z.; Wang, J. Measurement and Correlation of Solubilities of 3-Nitro-1,2,4-triazol-5-one (NTO) in 10 Pure Solvents and 3 Binary Solvents from 278.15 to 328.15 K. *J. Chem. Eng. Data* **2021**, *66*, 3897–3910. [[CrossRef](#)]
23. Noubigh, A. Stearic acid solubility in mixed solvents of (water + ethanol) and (ethanol + ethyl acetate): Experimental data and comparison among different thermodynamic models. *J. Mol. Liq.* **2019**, *296*, 112101. [[CrossRef](#)]

24. Yang, C.; Li, Q.; Wu, Y. Thermodynamic models for determination of solid-liquid equilibrium of the 4-methylbenzoic acid in pure and binary organic solvents. *J. Mol. Liq.* **2017**, *238*, 432–439. [[CrossRef](#)]
25. Ouyang, J.; Liu, L.; Zhou, L.; Liu, Z.; Li, Y.; Zhang, C. Solubility, dissolution thermodynamics, Hansen solubility parameter and molecular simulation of 4-chlorobenzophenone with different solvents. *J. Mol. Liq.* **2022**, *360*, 119438. [[CrossRef](#)]
26. Zhou, G.; Chen, K.; Yang, Z.; Shao, D.; Fan, H. Solubility and Thermodynamic Model Correlation of Zonisamide in Different Pure Solvents from T = (273.15 to 313.15) K. *J. Chem. Eng. Data* **2020**, *65*, 3637–3644. [[CrossRef](#)]
27. Shan, Y.; Luo, J.; Shi, C.; Li, J.; Yu, Q. Measurement and Correlation of Solubility Data for Cytosine in Fourteen Pure Solvents from 288.15 to 328.15 K. *J. Chem. Eng. Data* **2022**, *67*, 3299–3309. [[CrossRef](#)]
28. Yin, Y.; Bao, Y.; Gao, Z.; Wang, Z.; Liu, D.; Hao, H.; Wang, Y. Solubility of Cefotaxime Sodium in Ethanol + Water Mixtures under Acetic Acid Conditions. *J. Chem. Eng. Data* **2014**, *59*, 1865–1871. [[CrossRef](#)]
29. Ye, Y.-j.; Xia, X.-q.; Dai, X.-t.; Huang, C.-h.; Guo, Q. Effects of temperature, salinity, and pH on 222Rn solubility in water. *J. Radioanal. Nucl. Chem.* **2019**, *320*, 369–375. [[CrossRef](#)]
30. Huang, W.; Wang, H.; Li, C.; Wen, T.; Xu, J.; Ouyang, J.; Zhang, C. Measurement and correlation of solubility, Hansen solubility parameters and thermodynamic behavior of Clozapine in eleven mono-solvents. *J. Mol. Liq.* **2021**, *333*, 115894. [[CrossRef](#)]
31. Li, W.; Wang, L.; Shi, P.; Gao, Z. Determination and Correlation of Solubility of Forms I and II of Imidacloprid in Seven Pure Solvents from 293.15 to 333.15 K. *J. Chem. Eng. Data* **2020**, *65*, 5421–5427. [[CrossRef](#)]
32. Mou, M.; Jiang, M. Fast Continuous Non-Seeded Cooling Crystallization of Glycine in Slug Flow: Pure α -Form Crystals with Narrow Size Distribution. *J. Pharm. Innov.* **2020**, *15*, 281–294. [[CrossRef](#)]
33. Leng, F.; Zhou, S.; Li, S.; Xu, M.; Zhang, K.; Guo, T.; Chen, T.; Yang, P. Solubility, Crystallization, and Characterization of Cytidine Sulfate. *ACS Omega* **2023**, *8*, 25288–25294. [[CrossRef](#)] [[PubMed](#)]
34. Constance, E.N.; Mohammed, M.; Mojibola, A.; Egiefameh, M.; Daodu, O.; Clement, T.; Ogundolie, T.; Nwawulu, C.; Aslan, K. Effect of Additives on the Crystal Morphology of Amino Acids: A Theoretical and Experimental Study. *J. Phys. Chem. C* **2016**, *120*, 14749–14757. [[CrossRef](#)]

Disclaimer/Publisher's Note: The statements, opinions and data contained in all publications are solely those of the individual author(s) and contributor(s) and not of MDPI and/or the editor(s). MDPI and/or the editor(s) disclaim responsibility for any injury to people or property resulting from any ideas, methods, instructions or products referred to in the content.